



Article

Transcription Factor SiDi19-3 Enhances Salt Tolerance of Foxtail Millet and *Arabidopsis*

Shenghui Xiao [†], Yiman Wan [†], Shiming Guo, Jiayin Fan, Qing Lin, Chengchao Zheng and Changai Wu ^{*†}

State Key Laboratory of Crop Biology, College of Life Sciences, Shandong Agricultural University, Tai'an 271018, China

* Correspondence: cawu@sdau.edu.cn

[†] These authors contributed equally to this work.

Abstract: Salt stress is an important limiting factor of crop production. Foxtail millet (*Setaria italica* L.) is an important model crop for studying tolerance to various abiotic stressors. Therefore, examining the response of foxtail millet to salt stress at the molecular level is critical. Herein, we discovered that SiDi19-3 interacts with SiPLATZ12 to control salt tolerance in transgenic *Arabidopsis* and foxtail millet seedlings. *SiDi19-3* overexpression increased the transcript levels of most Na⁺/H⁺ antiporter (*NHX*), salt overly sensitive (*SOS*), and calcineurin B-like protein (*CBL*) genes and improved the salt tolerance of foxtail millet and *Arabidopsis*. Six *SiDi19* genes were isolated from foxtail millet. Compared with roots, stems, and leaves, panicles and seeds had higher transcript levels of *SiDi19* genes. All of them responded to salt, alkaline, polyethylene glycol, and/or abscisic acid treatments with enhanced expression levels. These findings indicate that *SiDi19-3* and other *SiDi19* members regulate salt tolerance and other abiotic stress response in foxtail millet.

Keywords: *CBLs*; *Di19-3*; *NHXs*; foxtail millet; salt tolerance; *SOSs*



Citation: Xiao, S.; Wan, Y.; Guo, S.; Fan, J.; Lin, Q.; Zheng, C.; Wu, C. Transcription Factor SiDi19-3 Enhances Salt Tolerance of Foxtail Millet and *Arabidopsis*. *Int. J. Mol. Sci.* **2023**, *24*, 2592. <https://doi.org/10.3390/ijms24032592>

Academic Editor: Yong-Hwan Moon

Received: 10 December 2022

Revised: 12 January 2023

Accepted: 26 January 2023

Published: 30 January 2023



Copyright: © 2023 by the authors. Licensee MDPI, Basel, Switzerland. This article is an open access article distributed under the terms and conditions of the Creative Commons Attribution (CC BY) license (<https://creativecommons.org/licenses/by/4.0/>).

1. Introduction

Salt stress affects physiological factors such as plant growth, development, and yield [1–3]. Plants acquire various molecular, biochemical, and physiological responses to tolerate salt stress [1]. Re-establishing ionic equilibrium to enhance salt tolerance is a crucial process for plants [4]. Additionally, the salt overly sensitive (*SOS*) pathway plays an important role in the response to salt stress in plants. The plasma membrane-localized Na⁺/H⁺ antiporter *SOS1* and its regulatory proteins, including *SOS2* (a protein kinase, also known as *CIPK24*), *SOS3*/calcineurin B-like protein 4 (*CBL4*), and other *CBL* proteins, maintain this process [5–8]. Under salt stress, *SOS3* and *CBL10* collaborate in the roots and shoots to detect the rise in cytoplasmic calcium and transmit this signal to the downstream serine/threonine protein kinase *SOS2*. Subsequently, *SOS2* phosphorylates *SOS1* to enhance Na⁺/H⁺ exchange activity and improve plant salt tolerance [1,3]. Simultaneously, tonoplast-localized Na⁺/H⁺ antiporters (*NHXs*) that sequester Na⁺ within vacuoles also play vital roles in re-establishing ionic homeostasis under salt stress [9,10]. Loss of function of *SOS* and *NHX* genes results in hypersensitivity to salt stress owing to high Na⁺ accumulation in the cytosol. In contrast, overexpression of the products of these genes improves salt tolerance owing to the low Na⁺ accumulation in the cytosol.

The Cys2/His2-type zinc-finger protein motif was first identified in transcription factor IIIA from *Xenopus laevis* which can be induced by drought stress [11–13]. Proteins containing the Cys2/His2-type zinc-finger are one of the best-characterized DNA-binding transcription factors in eukaryotes [14]. Di19 (drought induced) protein was firstly isolated from drought treated *Arabidopsis* roots [15]. All seven of the *AtDi19* proteins contain two atypical Cys2/His2-type zinc-finger motifs [13]. Every member of the *AtDi19* family, except *AtDi19-2*, has putative nuclear localization signals (NLS), and all but two are localized in

the nucleus [13]. Dehydration quickly stimulates the expression of *AtDi19-1* and *AtDi19-3*; however, high-salt stress induces the expression of *AtDi19-2* and *AtDi19-4* [13], indicating the different roles of *AtDi19* members in abiotic stress responses. By binding to the TACA(A/G)T element in the promoters of pathogenesis-related 1 (*PR1*), *PR2*, and *PR5* genes, *AtDi19-1* contributes to the response of plants to drought stress [14]. Transgenic *Arabidopsis* plants are more sensitive to salt, drought, oxidative, and abscisic acid (ABA) stressors when *GmDi19-5* is overexpressed [16]. Additionally, *GhDi19-1* and *GhDi19-2* are implicated in ABA signal transduction and plant responses to salt and drought stresses [17]. *ZmDi19-1* overexpression enhances salt tolerance in *Arabidopsis* by affecting the expression of stress-related genes [18]. The importance of *TaDi19A* in abiotic stress has been discussed, along with some potential modes of action [19]. By directly interacting with the promoter of *DREB2A* in rice, *OsDi19-4* acts downstream of *OsCDPK14* to positively control ABA response [20]. Furthermore, *PheDi19-8* directly binds to the promoter of *DREB2A*, and *PheCDPK22* overexpression increases *Arabidopsis* sensitivity to drought stress [21]. Overexpression of *PtDi19-2* and *PtDi19-7* increased ABA sensitivity and drought tolerance in *Arabidopsis* [22]. *PtDi19-2* and *PtDi19-7* probably influence the ability of transgenic plants to withstand drought via ABA-dependent signaling pathways [22]. Therefore, *Di19* proteins play a crucial role in the responses of various plant species to abiotic stressors. However, whether *Di19* proteins control the salt stress response by regulating the SOS pathway remains unclear.

An earliest cultivated cereal crop, foxtail millet, is mostly farmed in northern China and other parts of East Asia. This is a ubiquitous crop growing in various environments [23–26]. However, the response of foxtail millet plants to salt stress remains unclear. We previously discovered that *AtPLATZ2* interacts with *AtDi19-3* in yeast two-hybrid tests and adversely affects the salt tolerance of *Arabidopsis* by suppressing the expression of *CBL4/SOS3* and *CBL10/SCaBP8* [27], thereby indicating the role of *AtDi19-3* in salt stress responses in *Arabidopsis*. Similarly, we discovered that *SiPLATZ12* from foxtail millet inhibits the expression of the majority of *SOS*, *CBL*, and *NHX* genes, thereby adversely affecting salt tolerance [28]. However, whether *SiPLATZ12* interacts with *SiDi19-3* to regulate salt tolerance of foxtail millet is unclear. In this study, we verified the interaction of *SiDi19-3* with *SiPLATZ12* and the function of *SiDi19-3* in the salt stress response in foxtail millet and *Arabidopsis*. Furthermore, the effects of *SiDi19-3* on the expression of *SiNHXs/AtNHXs*, *SiSOSs/AtSOSs*, and *SiCBLs/AtCBLs* were investigated in transgenic foxtail millet and *Arabidopsis*. The *SiDi19* family was also isolated, and their expression in specific tissues and in response to specific stimuli was determined. Our findings revealed a new positive regulator of the majority of *SOS*, *CBL*, and *NHX* genes that improve plant salt tolerance.

2. Results

2.1. *SiDi19-3* Interacts with *SiPLATZ12*

First, we created *SiDi19-3*-green fluorescence protein (GFP) transgenic hairy roots of foxtail millet. The GFP signal was particularly observed to be merged with the 4',6-diamidino-2-phenylindole (DAPI) dye, indicating the nuclear localization of *SiDi19-3* in the transgenic hairy roots. We then examined whether *SiDi19-3* and *SiPLATZ12* interacted. Yeast cells co-transformed with the *SiPLATZ12*-AD and *SiDi19-3*-BD constructs were able to grow in a synthetic medium deficient in Trp, Leu, His, and 25 mM AbA (aureobasidin A) (quadruple dropout [QDO]), indicating the physical interaction between *SiPLATZ12* and *SiDi19-3* in yeast cells (Figure 1B). In the pull-down assays, *SiPLATZ12*-His could be pulled down by *SiDi19-3*-GST but not by GST alone (Figure 1C). Bimolecular fluorescence complementation (BiFC) assays were carried out. The YFP signal was observed using a confocal microscope when *SiPLATZ12* fused to C-terminus of YFP (*SiPLATZ12*-CYFP) and *SiDi19-3* fused to N-terminus of YFP (*SiDi19-3*-NYFP) were co-transformed into tobacco epidermis cells; however, no YFP signals were observed when *SiPLATZ12*-CYFP and NYFP, *SiDi19-3*-NYFP, and CYFP, or NYFP and CYFP were co-transformed (Figure 1D). The YFP

signal could also be merged with the DAPI dye. These findings indicate an interaction between SiDi19-3 and SiPLATZ12.

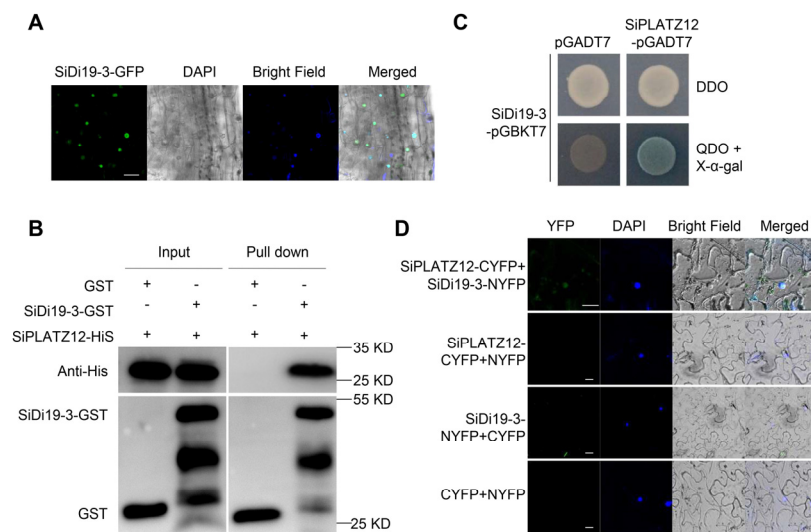


Figure 1. SiDi19-3 interacts with SiPLATZ12. (A) Subcellular localization of SiDi19-3 in transgenic hairy-roots of foxtail millet. The photographs were taken using the green channel (GFP fluorescence), blue channel (DAPI fluorescence), bright channel, and their combination under a confocal microscope. Scale bar = 20 μ m. (B) The SiDi19-3 and SiPLATZ12 interaction tested using yeast two-hybrid assay. DDO, Synthetic Dropout/-Leu-Trp; QDO, Synthetic Dropout/-Leu-Trp-His-Ade. (C) The SiDi19-3 and SiPLATZ12 interaction using in vitro pull-down assays. SiPLATZ12-His was incubated with GST or GST-SiDi19-3 purified from *E.coli* and was washed to remove unbound proteins. The bound proteins were eluted and analyzed using immunoblotting with anti-GST and anti-His antibodies. (D) The SiDi19-3 and SiPLATZ12 interaction in *N. benthamiana* indicated in bimolecular fluorescence complementation (BiFC) assay. DAPI, nuclear dye, 4',6-diamidino-2-phenylindole. The photographs were taken using the green channel (YFP fluorescence), blue channel (DAPI fluorescence), bright channel, and their combination under a confocal microscope. Scale bars = 20 μ m.

2.2. SiDi19-3 Enhances Salt Tolerance of Foxtail Millet

To analyze the role of *SiDi19-3* under salt stress, we overexpressed *SiDi19-3* in the hairy roots of 'Yugu1' seedlings using K599 agrobacterium-mediated transformation. Notably, the *SiDi19-3* transcript levels in transgenic foxtail millet seedlings were higher than those in the control (Em, empty vector transgenic seedlings) (Figure 2A). The *35S::SiDi19-3* and Em transgenic seedlings were grown in the same way under typical conditions. In *35S::SiDi19-3* transgenic seedlings under salt stress, primary root length was significantly greater and root fresh weight was higher than those in control seedlings (Figure 2B–D), demonstrating that SiDi19-3 positively controls the salt tolerance of foxtail millet seedlings.

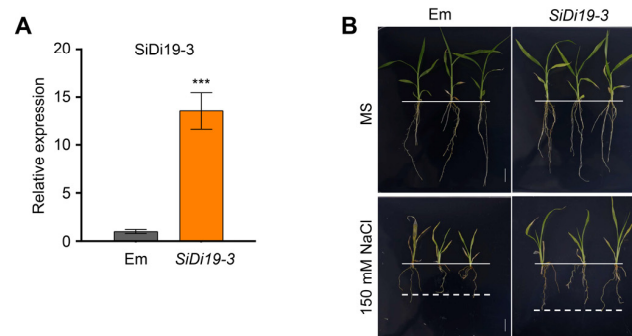


Figure 2. Cont.

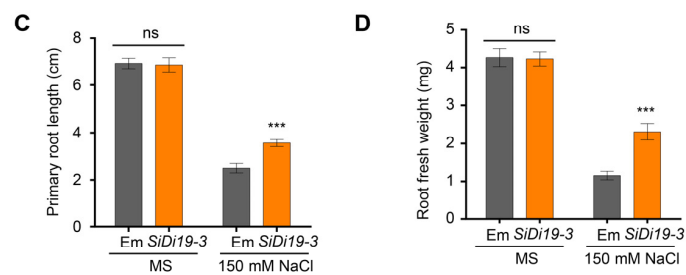


Figure 2. Overexpression of *SiDi19-3* enhances salt tolerance of foxtail millet seedlings. (A) Relative expression of *SiDi19-3* in *35S::SiDi19-3* transgenic hairy-roots of foxtail millet seedlings. The empty vector (Em) was used as a control. *SiACTIN7* and *18S rRNA* were used as two normalizing expression values within the calculation leading to the relative expression values. Data shown are means of three biological replicates. At least 30 seedlings were used for each replicate. Data represent the mean \pm SEM of three biological repeats. Student's *t*-test indicated the significance at *** $p < 0.001$ levels. (B) Phenotypes of *35S::SiDi19-3* and Em transgenic foxtail millet seedlings with or without salt stress. Scale bars = 1 cm. (C) Primary root length and (D) root fresh weight of foxtail millet seedlings grown under salt stress or in control conditions. Data represent the mean \pm SEM of three biological repeats. Student's *t*-test indicated significance at *** $p < 0.001$ level. ns, no significance.

2.3. *SiDi19-3* Increases the Expression of *SiSOS*, *SiCBL*, and *SiNHX* Genes

To better understand how *SiDi19-3* controls the salt stress response in foxtail millet seedlings, we evaluated the transcript levels of salt tolerance related genes, including *SiSOSs*, *SiCBLs*, and *SiNHXs* (Figure 3). Under salt stress, compared to the Em transgenic foxtail millet seedlings, *SiDi19-3*-overexpression seedlings raised the transcript levels of all *SiCBLs*, except *SiCBL5* and *SiCBL6*; all *SiNHXs*, except *SiNHX3*; *SiSOS1*; and *SiSOS2*. However, under normal conditions, *SiDi19-3* overexpression did not alter the transcript levels of them. These findings implied that the majority of the analyzed *NHX*, *SOS*, and *CBL* genes were upregulated by *SiDi19-3* under salt stress.

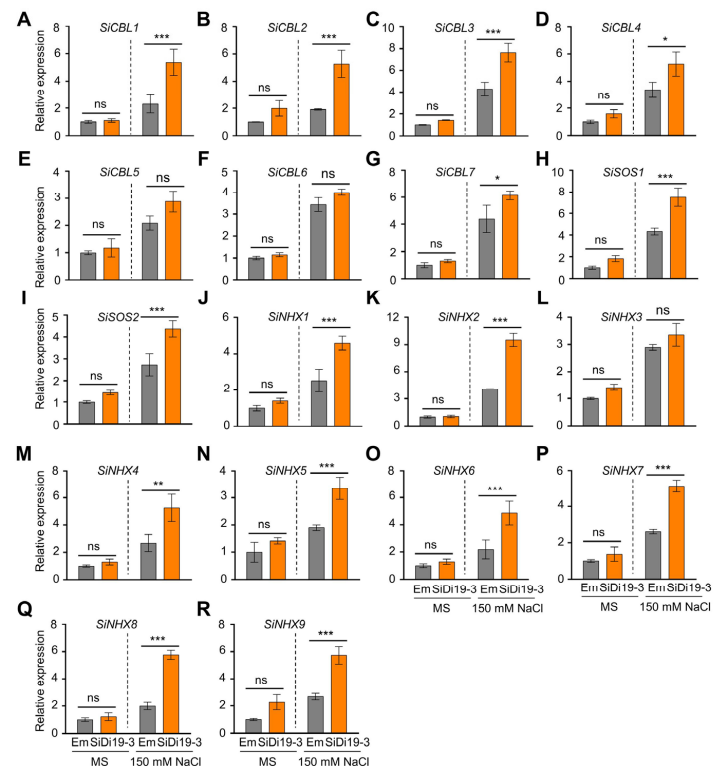


Figure 3. *SiDi19-3* upregulates the expression of salt tolerance related genes in foxtail millet. Relative

expression levels of *SiCBL1-7* (A–G), *SiSOS1-2* (H,I), and *SiNHX1-9* (J–R) in transgenic foxtail millet hairy roots treated with 150 mM NaCl for 24 h or not. *SiACTIN7* and *18S rRNA* were used as two normalizing expression values within the calculation leading to the relative expression values. Data shown are means of three biological replicates. Data represent the mean \pm SEM of three biological repeats. Student's *t*-test showed the significance at * $p < 0.05$, ** $p < 0.01$, and *** $p < 0.001$ levels. ns, no significance.

2.4. Heterologous Expression of *SiDi19-3* Increases Salt Tolerance of *Arabidopsis*

To confirm its function, *SiDi19-3* was heterologously expressed in *Arabidopsis thaliana* Col-0 plants. Transgenic *Arabidopsis* lines #1, #3, and #4 indicated higher *SiDi19-3* transcript levels (Figure 4A). Under salt stress, the *SiDi19-3* transgenic *Arabidopsis* exhibited faster germination rate and growth with higher fresh weight and longer primary root length than those of the wild type (WT; Figure 4B–F). Furthermore, expression of *SiDi19-3* increased the expression of *AtCBL1-10* and *AtSOS1-2* but not *AtCBL5* in *Arabidopsis* seedlings under salt stress (Figure 5). Under normal conditions, no change was observed in germination rate, fresh weight, and primary root length nor in the expression of *NHXs*, *SOSs*, and *CBLs* in *Arabidopsis*. These results demonstrated that *SiDi19-3* also acts as a positive regulator of salt stress in *Arabidopsis*.

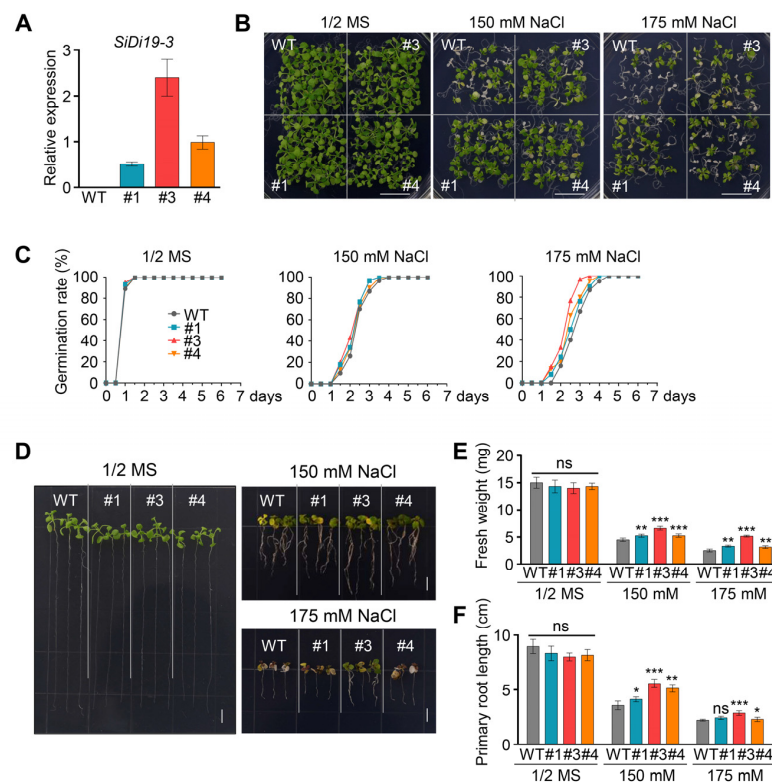


Figure 4. Overexpression of *SiDi19-3* enhances salt tolerance of transgenic *Arabidopsis*. (A) *SiDi19-3* transcript levels in wild type (WT) and *SiDi19-3* transgenic *Arabidopsis*. (B,C) Phenotypes and germination rate of WT and *SiDi19-3* transgenic *Arabidopsis* seeds cultured on half-strength (1/2) MS medium containing 150 mM and 175 mM NaCl or in control conditions. At least 50 seeds were used for each replicate. Three biological repeats were performed. Scale bars = 1 cm. (D) Phenotypes of 3-day-old uniformly developed seedlings of WT and three *SiDi19-3* transgenic *Arabidopsis* seedlings grown on 1/2 MS medium with or without 150 mM and 175 mM NaCl for 14 days. Scale bars = 1 cm. (E,F) Fresh weight and primary root length of WT and *SiDi19-3* transgenic *Arabidopsis* seedlings treated as described in (D). At least 30 seedlings were used for each replicate. Data shown are means of three biological replicates. Data represent means \pm SEM of three replicates. Student's *t*-test indicated the significance at * $p < 0.05$, ** $p < 0.01$, and *** $p < 0.001$ levels. ns, no significance.

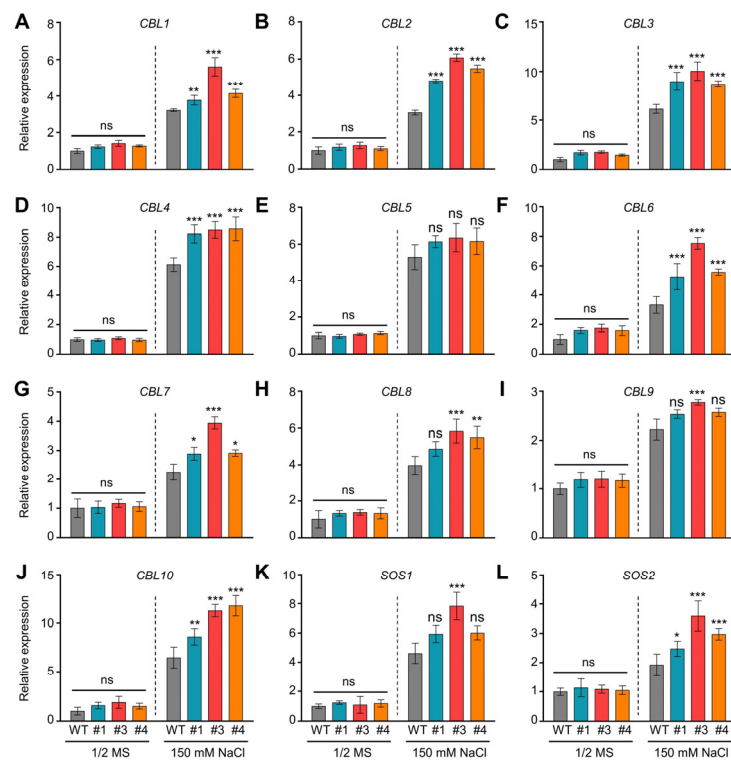


Figure 5. SiDi19-3 affects the expression of salt tolerance related genes in *Arabidopsis*. Expression levels of CBL (A–J) and SOS (K,L) genes in wild type (WT) and SiDi19-3 transgenic *Arabidopsis* seedlings treated with 200 mM NaCl for 24 h or not. *AtGAPDH* and *AtUBQ10* were used as two normalizing expression values within the calculation leading to the relative expression values. Data shown are means of three biological replicates. Data represent the mean \pm SEM of three biological repeats. Student's *t*-test indicated the significance at * $p < 0.05$, ** $p < 0.01$, and *** $p < 0.001$ levels. ns, no significance.

2.5. Identification of SiDi19 Gene Family in Foxtail Millet

To determine whether other SiDi19 members in foxtail millet exhibited a similar response to salt stress and other abiotic stressors, we searched the 'Yugu1' genome assembly containing Di19 sequences from foxtail millet (Supplemental Table S1). We found that SiDi19 genes were unevenly distributed among nine chromosomes (chr) in foxtail millet. In comparison, chr3 contained three SiDi19 genes, chr5 had two, and chr1 had only one SiDi19 gene. Based on their chromosomal placement, the SiDi19 genes were named SiDi19-1—SiDi19-6 (Figure 6A). A bioinformatical neighbor-joining tree analysis divided Di19 genes from *Setaria italica*, *Oryza sativa*, *Sorghum bicolor*, *Zea mays*, *Glycine max*, and *Arabidopsis* into three subfamilies that were similar to each other (Figure 6B), indicating that Di19 probably plays conserved roles among plant species. According to gene structural analysis, all SiDi19 genes had the same structure, consisting of five variable-length exons and four introns (Figure 6C). It is interesting that all Di19 proteins have two conserved motifs except SiDi19-6, which indicate that they may have similar biological functions and that SiDi19-6 protein might play a distinct function in plants (Figure 6D).

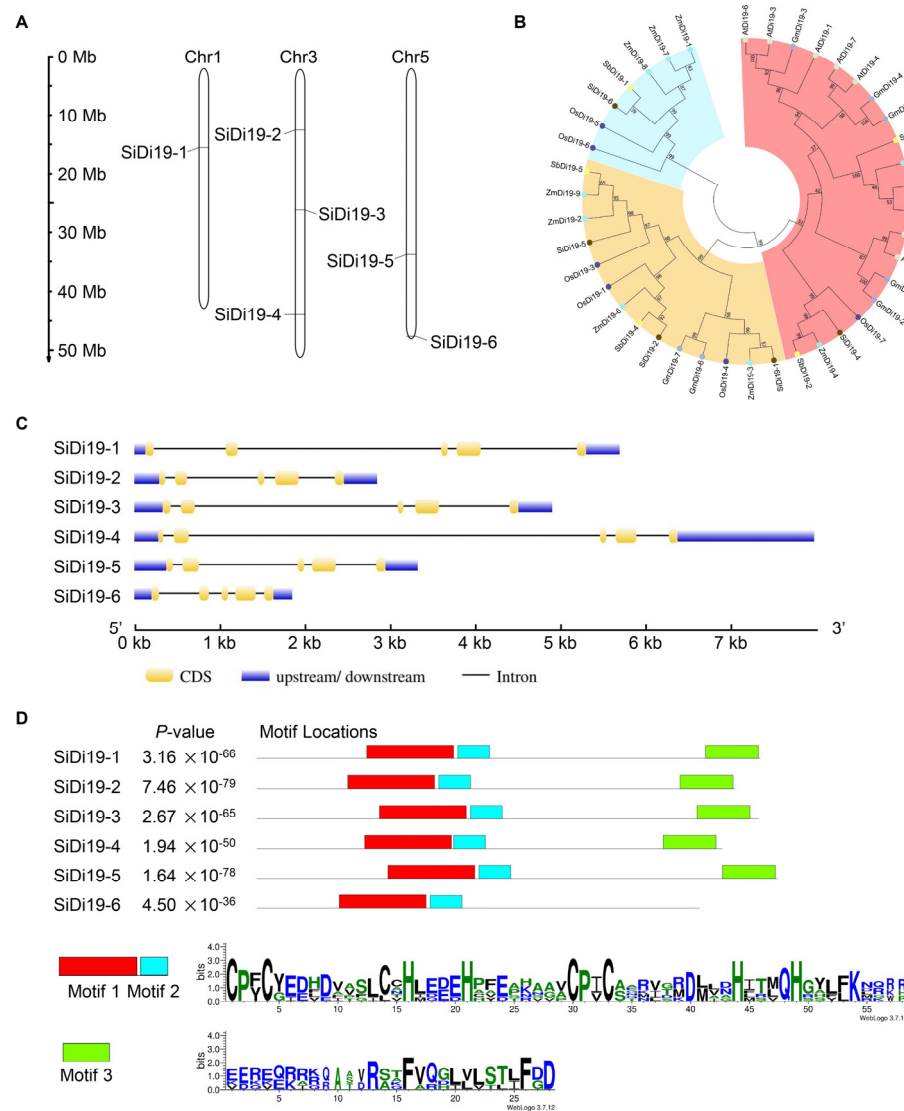


Figure 6. Analysis of *SiDi19* genes in foxtail millet. (A) Distribution of *SiDi19-3* genes on the chromosomes of foxtail millet. (B) The tree was reconstructed based on the highly conserved zf-Di19 domain of Di19 proteins in *Setaria italica*, *Oryza sativa*, *Arabidopsis*, *Sorghum bicolor*, and *Zea mays*. Bootstrap values from 1000 replicates are indicated at each node of the branches. (C) Gene structures of six *SiDi19* genes in foxtail millet created at GSDS website. (D) Conserved motif analysis according to multiple sequence alignments of *SiDi19* proteins using the MEME website.

2.6. Expression Patterns of *SiDi19* Genes

Next, using quantitative reverse transcription polymerase chain reaction (RT-qPCR) analysis, we examined the transcriptional levels of *SiDi19* genes in various organs. *SiDi19-1*, *SiDi19-4*, and *SiDi19-6* indicated higher transcript levels in stems than other members of the gene family, whereas *SiDi19-2*, *SiDi19-3*, and *SiDi19-4* were preferentially expressed in seeds (Figure 7A). Furthermore, *SiDi19-1*, *SiDi19-3*, and *SiDi19-4* indicated higher transcript levels in the panicles than other plant parts. All six *SiDi19* genes had low transcript levels in the roots and leaves. These gene expression patterns in different tissues suggested that some members may function redundantly at different developmental stages.

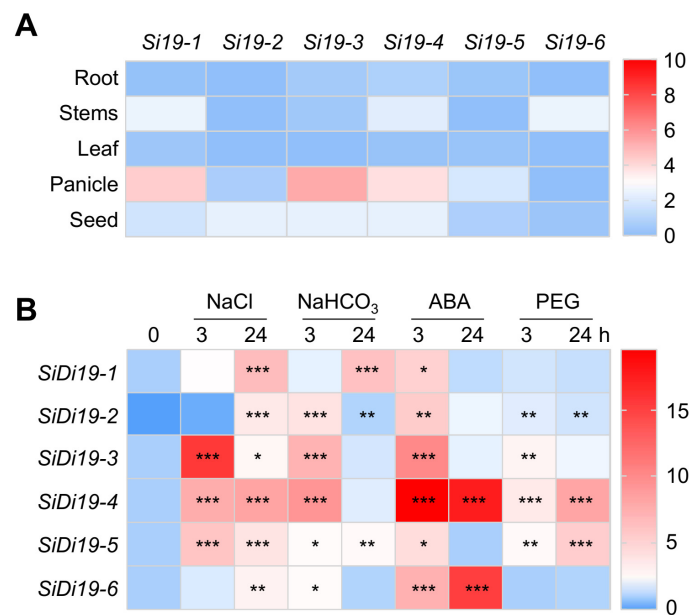


Figure 7. Expression patterns of *SiDi19* gene members in foxtail millet. **(A)** Quantitative reverse transcription polymerase chain reaction (RT-qPCR) analysis of *SiDi19* genes in roots, stems, leaves, panicles, and seeds. Root, stem, and leaf samples were collected from ten uniformly developed 14-day-old seedlings. Five approximately 5-cm-long, uniformly developed panicles from two-month-old Yugu1 seedlings were collected. Thirty mature seeds were collected. Each tissue sample was pooled and ground, and, respectively, three 100 mg tissue powder were weighed to extract RNA for RT-qPCR. All the tissues were collected three times from different plants for the three biological replicates. **(B)** RT-qPCR analysis of *SiDi19* genes in 7-day-old Yugu1 seedlings after treatment with 200 mM NaCl, 50 mM NaHCO₃, 100 μM ABA, or 20% PEG6000 for 0, 3, and 24 h. *SiACTIN7* and *18S rRNA* were used as two normalizing expression values within the calculation leading to the relative expression values. Data shown are means of three biological replicates. Data represent the mean ± SEM of three biological repeats. Student's *t*-test indicated the significance at * $p < 0.05$, ** $p < 0.01$, and *** $p < 0.001$ levels.

We initially examined the *cis*-elements in the promoters of *SiDi19* genes to determine whether any *SiDi19* genes other than *SiDi19-3* operated in response to abiotic stresses (Supplemental Table S2). Two or more ABA-responsive elements (ABREs) were predicted for all *SiDi19* promoters. An auxin-responsive element (TGA) was predicted in the promoters of *SiDi19-1*, -3 and -5. Two or three ethylene response elements (ERFs) were predicted in the promoters of *SiDi19-2* and -3. More than one drought responsive element (DRE/MBS) was predicted in the promoters of *SiDi19-1*, -2, -4, and -6. One or two low-temperature responsive elements (LTRs) were predicted in the promoters of *SiDi19-2* to -5. One to three salicylic acid-responsive elements (TCA/SARE) were predicted in the promoters of *SiDi19-1* and -3, respectively. More than one wound responsive element (WRE) was predicted in the promoters of all *SiDi19* genes except *SiDi19-2*. These results suggest the potential roles of *SiDi19* genes in hormone-mediated abiotic stress responses.

Furthermore, we detected the transcript levels of the *SiDi19* genes at 3 and 24 h after appropriate treatments. As depicted in Figure 7B, some treatments clearly induced the expression of several *SiDi19* genes. For example, all *SiDi19* genes were induced by NaCl, NaHCO₃, and ABA treatments at 3 or 24 h, and all *SiDi19* genes, except *SiDi19-6*, were induced by PEG. Furthermore, *SiDi19-3* and -4 indicated the highest inducible levels in response to NaCl and ABA treatments. These results indicate the redundant roles of *SiDi19* genes in response to multiple ABA-mediated abiotic stresses in foxtail millet.

3. Discussion

Di19 members of several species control various abiotic stresses. Some constituents effectively controlled resistance to drought stress. For instance, AtDi19 improves drought tolerance in transgenic *Arabidopsis* [14]. In addition to AtDi19, OsDi19-4 [20], ZmDi19-1 [18], PheDi19-8 [21], and PtDi19-2/-7 [22] have similar functions. However, some Di19 adversely influence drought tolerance, such as TaDi19A [19], AtDi19-3 [29], and GmDi19-5 [16]. Additionally, ZmDi19-1 positively regulates salt tolerance [18], whereas AtDi19-3 [29], TaDi19A [19], GmDi19-5 [16], GhDi19-1, and GhDi19-2 [17] negatively regulate salt tolerance. Whether foxtail millet *Di19* genes function in response to abiotic stress is unknown. In this study, we discovered that SiDi19-3 favorably regulates the salt tolerance in foxtail millet and *Arabidopsis* (Figures 2 and 4). Notably, both *SiDi19-3* and *SiDi19-4* displayed comparable expression patterns, including high transcript levels in the panicles and seeds, and exhibited similar responses to salt, alkaline, drought, and ABA treatments (Figure 7). These findings demonstrate that *Di19* genes play conserved roles in abiotic stress response across plant species. Furthermore, *SiDi19-3* and *SiDi19-4* probably control the development of panicles and seeds in foxtail millet; further studies are warranted to ascertain this since the involvement of *Di19* in plant development has not yet been reported. Further studies revealed that Di19 interacted with several proteins. Our previous report indicated that AtDi19-3 interacted with AtPLATZ2 [27]. Herein, we demonstrate that SiDi19-3 and SiPLATZ12 interacted with each other (Figure 1B–D). Both SiPLATZ12 and AtPLATZ2 exhibited detrimental roles in regulating plant salt stress [27,28]. However, SiDi19-3 positively regulates salt tolerance in foxtail millet and transgenic *Arabidopsis* (Figures 2 and 4), whereas AtDi19-3 negatively controls salt tolerance in *Arabidopsis* [29]. In addition, AtDi19-3 interacts with AtIAA14, OsDi19-5, and OsIAA13 to control root elongation in *Arabidopsis* and rice [30]. Overexpression of GmDi19-5 increased sensitivity of transgenic *Arabidopsis* plants to salt, drought, oxidative, and ABA stresses and regulated expression of several ABA/stress-associated genes [16]. OsDi19-4, but not OsDi19-7, physically interacts with other Di19 members in yeast [31]. Members of Di19 appear to differently regulate abiotic stress through their different interacting proteins. The variant sequences between three conserved motifs may play roles in the interaction with different proteins (Figure 6D). However, precise regulatory framework is lacking.

The Di19 proteins belong to the Cys2His2 type transcription factor family, which regulates the expression of numerous genes involved in abiotic stress through the DNA-binding Cys2/His2 motifs [14]. For example, AtDi19-1 directly binds to the promoters of *PR1*, *PR2*, and *PR5* to regulate their expression in response to drought stress [14]. Similarly, AtDi19-3 positively controls the expression of *NIT1*, *ILL5*, *YUCCA*, *AUX1*, and *MYB77* [30]. By directly binding to the promoters of *OsASPG1* and *OsNAC18*, OsDi19-4 modulates the expression of ABA-responsive genes in rice [20]. In response to salt stress, ZmDi19-1 affects the expression of several stress-related genes, including *PR*, *RAB18*, *PDF*, and *COR15A* [18]. In contrast, the expression of *SOS2*, *ABI1/5*, *ABF3/4*, *RD29A/B*, *RD22*, and *DREB2A* is repressed by TaDi19A [19], AtDi19-3 [29], GmDi19-5 [16], and PheDi19-8 [21]. We found for the first time that SiDi19-3 localizes in the nucleus when expressed in hairy roots of foxtail millet (Figure 1A) and elevates the expression of the majority of the analyzed *SOS*, *CBL*, and *NHX* genes under salt stress (Figures 3 and 5). Thus, SiDi19-3, similar to other Di19 members, controls the expression of many genes.

SiDi19-3 can control cytoplasmic Na⁺ homeostasis. *SOSs*, *CBLs*, and *NHXs* are important for cytoplasmic Na⁺ homeostasis. In *Arabidopsis*, SOS2-SOS3 (CBL4)/SCaBP8 (CBL10) complexes activate the transporter activities of *SOS1* and *NHXs* [5,32,33]. The results indicated that SiDi19-3 increased the expression of the majority of the analyzed *SOS*, *CBL*, and *NHX* genes (Figures 3 and 5), indicating the involvement of SiDi19-3 in regulating cytoplasmic Na⁺ homeostasis. SiCBL4 and SiCIPK24 interact to attract SiCIPK24 to the plasma membrane. Compared with WT plants, SiCIPK24 transgenic *Arabidopsis* plants are more resilient to salt stress [34]. SiCBL5-overexpressing foxtail millet plants demonstrate increased tolerance to salt stress. Furthermore, SiCBL5-SiCIPK24 affects SiSOS1 function

in yeast cells [35]. We previously demonstrated that overexpression of *SiNHX2*, *SiCBL4*, and *SiCBL7* in the hairy roots of foxtail millet seedlings improved salt tolerance [28]. The salt tolerance of foxtail millet correlates with the expression of *SiNHX1* to *SiNHX4* [28]. Therefore, *SiDi19-3* mediates salt tolerance by maintaining cytoplasmic Na^+ homeostasis.

The development of foxtail millet might be influenced by *SiDi19-3*. Additionally, *NHXs* play roles in *Arabidopsis* stomatal control [36], plant growth [9,10,37], silique and seed development [38,39], and vacuolar K^+ and pH homeostasis [9,10]. The up-regulation of *SOS*, *CBL*, and *NHX* gene expression by *SiDi19-3* under salt stress (Figures 3 and 5) indicates that *SiDi19-3* may be involved in controlling foxtail millet growth and development under salt stress. The *SiDi19-3* transcript levels were higher in the panicles and in response to drought and ABA treatments (Figure 7), also indicating the possible participation of *SiDi19-3* in foxtail millet panicle or seed development and drought response. These roles of *SiDi19-3* and the underlying mechanisms merit additional studies.

4. Materials and Methods

4.1. Plant Materials and Growth Conditions

For investigation of gene expression and function, the foxtail millet (*S. italica*) cultivar 'Yugu1' and *Arabidopsis* Col-0 were employed. Foxtail millet seeds underwent sodium hypochlorite sterilization, were washed three times, and then were germinated for three days at 25 °C. Seven-day-old 'Yugu1' seedlings were exposed to Hoagland solution containing 200 mM NaCl, 50 mM NaHCO_3 , 100 μM ABA, or 20% (*w/v*) polyethylene glycol 6000 (PEG6000) for 3 and 24 h, respectively, for inducible expression analyses. The seedlings were collected and frozen in liquid nitrogen as soon as possible. Roots, stems, and leaves from 14-day-old seedlings, panicles from 2-month-old seedlings, and seeds of 'Yugu1' were collected and immediately frozen in liquid nitrogen for tissue expression analyses. The previously described techniques were used to grow foxtail millet seedlings with transgenic hairy roots [40].

The *A. thaliana* Col-0 was used as WT. The previously described techniques were used to grown *Arabidopsis* plants [41]. During the seed germination stage, seeds were exposed to 150 mM NaCl in 1/2 MS medium for 7 d. In a span of 7 d, the germinated seeds with 2 cm roots and 1 cm green shoots were counted daily. To induce salt stress, three-day-old seedlings germinated from seeds that were not salt treated of each genotype were transferred to 1/2 MS media containing 150 or 175 mM NaCl for an additional 14 d, and the root lengths and fresh weight of whole seedlings were measured. Three biological replicates of each experiment were performed.

4.2. Yeast Two-Hybrid (Y2H) Assays

The interaction between *SiDi9-3* and *SiPLATZ12* was tested using the Matchmaker GAL4 two-hybrid system (Clontech) as previously described [42]. Full-length coding sequences (CDSs) of *SiDi9-3* and *SiPLATZ12* were cloned into the pGBKT7 (BD) and pGADT7 (AD) vectors, respectively. The yeast strain AH109 was co-transformed with those constructs. Leu–Trp–His–Ade (QDO) was used for interaction selection, while double dropout (DDO) medium supplemented without Leu or Trp was used to grow the transformed cells. Primers used in this experiment are listed in Supplemental Table S3.

4.3. Bimolecular Fluorescence Complementation (BiFC) Assays

For these assays, the coding regions of *SiDi19-3* and *SiPLATZ12* were amplified and cloned into pSPYNE-35S (NYFP) and pSPYCE-35S (CYFP) vectors to fuse them with the N- or C-terminal YFP, respectively. The resultant 35S::*SiDi19-3*-NYFP and 35S::*SiPLATZ12*-CYFP constructs were transformed into *Agrobacterium tumefaciens* GV3101. The 35S::P19 vector was co-transformed into three-week-old *N. benthamiana* leaves with 35S::*SiDi19-3*-NYFP and 35S::*SiPLATZ12*-CYFP, 35S::*SiDi19-3*-NYFP and CYFP, NYFP, 35S::*SiPLATZ12*-CYFP, NYFP, and CYFP. After 28 h of culture, the transformed tobacco leaves were monitored for

reconstituted YFP fluorescence using an LSM880 confocal microscopy (Zeiss, Germany). The primers used in this experiment are listed in Supplemental Table S3.

4.4. Pull-Down Assays

For these assays, the CDSs of *SiDi19-3* and *SiPLATZ12* were cloned into pGEX-4T-1 and pCold-TF vectors to generate *SiDi19-3*-GST and *SiPLATZ12*-His constructs, respectively, as previously described [41]. Subsequently, the constructs were transformed into competent Rosetta *E. coli* cells. *SiDi19-3*-GST and *SiPLATZ12*-His proteins were induced by IPTG and were then used for protein purification using the His-Tagged Protein Purification Kit (CW BIO, Beijing, China) and BeyoGold GST-tag Purification Resin (BeyoGold, Shanghai, China). Next, *SiDi19-3*-GST or GST proteins were incubated with *SiPLATZ12*-His protein in 300 μ L of binding buffer (P2262, Beyotime, Shanghai, China) for 1 h at 4 °C in a continuously rotator. The proteins were detected using immunoblotting with anti-GST or anti-His antibodies after elution from the beads. Signals were detected using a Chemiluminescence Imaging System (K4000, KCRX Biotechnology, Beijing, China). The primers used in this experiment are listed in Supplemental Table S3.

4.5. Subcellular Localization Analysis

The transgenic hairy-roots harboring p*SiDi19-3*:*SiDi19-3*-GFP were obtained using the previously described techniques [39] to analyze the subcellular location of *SiDi19-3*. LSM880 high-resolution laser confocal microscope (Zeiss, Germany) was utilized to view GFP fluorescence in the root tips of the transgenic hairy roots. The DAPI was used to detect the nuclear dye.

4.6. Generation of Transgenic Foxtail Millet and *Arabidopsis*

Under the control of the 35S promoter, the full-length CDS of *SiDi19-3* was amplified and cloned into PROKII vector. Based on an earlier study [39], the recombinant plasmid was transformed into *A. tumefaciens* K599. Positive transformants were inoculated into 20 mL of liquid solution and cultured with continuous shaking for 12 h. The culture was then centrifuged at 6000 \times g for 5 min. Subsequently, the cells were resuspended in 1/2 MS liquid medium to a final concentration with OD₆₀₀ = 1.0. Three-day-old shoot tips were cut and incubated with *A. tumefaciens* containing 35S::*SiDi19-3* or the empty vector at 28 °C for 10–20 min with continuous shaking. The transformed shoot tips were transferred onto 1/2 MS solid medium supplemented with 100 mg/L timentin overnight to induce root formation [39]. Approximately 7 d later, transgenic hairy roots were confirmed using RT-qPCR. Twenty transgenic seedlings were transferred into 1/2 MS liquid medium with or without 150 mM NaCl for an additional 7 d. The phenotype was photographed, and root length was measured. Three biological replicates of each experiment were performed.

Transgenic *Arabidopsis* containing 35S::*SiDi19-3* was simultaneously generated using the floral-dipping method as previously described [43]. T₃ transgenic *Arabidopsis* plants were selected using 1/2 MS medium supplemented with 50 mg/L kanamycin and confirmed by RT-qPCR using the primers listed in Supplemental Table S3.

4.7. Identification of *SiDi19* Genes in Foxtail Millet

Di19 family members from *Arabidopsis* were used to BLAST the foxtail millet genome in Phytozome V12 (<https://phytozome.jgi.doe.gov> (accessed on 19 April 2022)) to identify the *SiDi19* genes. The isoelectric point and molecular weight were predicted using ExPASy Proteomics Server (<http://expasy.org/> (accessed on 19 April 2022)). An evolutionary tree was generated using MEGA6 software and a phylogenetic evolutionary tree was constructed using neighbor-joining analysis and bootstrap method, with 1000 replicates. *Di19* genes from *Oryza sativa*, *Arabidopsis*, *Sorghum bicolor*, *Zea mays*, and *Glycine max* were previously identified [13,16,29]. The gene structures of *SiDi19* members were analyzed using the Gene Structure Display Server (GSDS; <http://gsds.cbi.pku.edu.cn/> (accessed on 19 April 2022)). MEME (<https://meme-suite.org/meme/tools/meme> (accessed on 19

April 2022)) was used to analyze the conserved motifs. The *cis*-elements in the promoters of the SiDi19 genes were predicted using PlantCARE (<http://bioinformatics.psb.ugent.be/webtools/plantcare/html/> (accessed on 19 April 2022)).

4.8. RNA Extraction and RT-qPCR

Total RNAs was extracted from the indicated tissues and seedlings treated with the indicated stimuli using RNAiso Plus (Takara, Ohtsu, Japan). Two micrograms of total RNAs were used to synthesize cDNAs using the PrimeScript™ RT reagent kit (TaKaRa, Ohtsu, Japan) according to the manufacturer's instructions. Further, RT-qPCR was performed using ChamQ Universal SYBR qPCR Master Mix (Vazyme, Biotech Co., Ltd.) in a three-step program on a CFX96™ Real-Time PCR Detection System (Bio-Rad, Hercules, CA, USA). *SiACTIN7* and 18S rRNA were used as two normalizing expression values within the calculation leading to the relative expression values in foxtail millet [40,44]. *AtGAPDH* and *AtUBQ10* were used as two normalizing expression values within the calculation leading to the relative expression values in *Arabidopsis* [41,42]. Three biological replicates were performed. The Primers used are listed in Supplementary Table S3.

Supplementary Materials: The following supporting information can be downloaded at: <https://www.mdpi.com/article/10.3390/ijms24032592/s1>.

Author Contributions: C.W. and S.X. conceived the experiments; S.X. and C.W. wrote the article; S.X., Y.W., S.G., J.F. and Q.L. performed the experiments; C.Z. provided suggestions. All authors have read and agreed to the published version of the manuscript.

Funding: This work was supported by the Central Guidance on Local Science and Technology Development Fund of Shandong Province (Grant number YDZX2021008), the Agricultural Fine Seed Project of Shandong Province (Grant number 2021LZGC006).

Institutional Review Board Statement: Not applicable.

Informed Consent Statement: Not applicable.

Data Availability Statement: The data and materials supporting the findings of this study are available from the corresponding author upon request.

Conflicts of Interest: The authors declare no conflict of interest.

References

1. Yu, Z.; Duan, X.; Luo, L.; Dai, S.; Ding, Z.; Xia, G. How plant hormones mediate salt stress responses. *Trends Plant Sci.* **2020**, *25*, 1117–1130. [[CrossRef](#)] [[PubMed](#)]
2. Zhou, Y.; Tang, N.; Huang, L.; Zhao, Y.; Tang, X.; Wang, K. Effects of salt stress on plant growth, Antioxidant Capacity, Glandular Trichome Density, and Volatile Exudates of *Schizonepeta tenuifolia* Briq. *Int. J. Mol. Sci.* **2018**, *19*, 252. [[CrossRef](#)] [[PubMed](#)]
3. Zhao, S.; Zhang, Q.; Liu, M.; Zhou, H.; Ma, C.; Wang, P. Regulation of plant responses to salt stress. *Int. J. Mol. Sci.* **2021**, *22*, 4609. [[CrossRef](#)] [[PubMed](#)]
4. Zhu, J.K. Regulation of ion homeostasis under salt stress. *Curr. Opin. Plant Biol.* **2003**, *6*, 441–445. [[CrossRef](#)]
5. Halfter, U.; Ishitani, M.; Zhu, J.K. The *Arabidopsis* SOS2 protein kinase physically interacts with and is activated by the calcium-binding protein SOS3. *Proc. Natl. Acad. Sci. USA* **2000**, *97*, 3735–3740. [[CrossRef](#)]
6. Liu, J.; Zhu, J.K. A calcium sensor homolog required for plant salt tolerance. *Science* **1998**, *280*, 1943–1945. [[CrossRef](#)]
7. Quintero, F.J.; Martinez-Atienza, J.; Villalta, I.; Jiang, X.; Kim, W.Y.; Ali, Z.; Fujii, H.; Mendoza, I.; Yun, D.J.; Zhu, J.K.; et al. Activation of the plasma membrane Na⁺/H⁺ antiporter Salt-Overly-Sensitive 1 (SOS1) by phosphorylation of an auto-inhibitory C-terminal domain. *Proc. Natl. Acad. Sci. USA* **2011**, *108*, 2611–2616. [[CrossRef](#)]
8. Zhou, X.; Li, J.; Wang, Y.; Liang, X.; Zhang, M.; Lu, M.; Guo, Y.; Qin, F.; Jiang, C. The classical SOS pathway confers natural variation of salt tolerance in maize. *New Phytol.* **2022**, *236*, 479–494. [[CrossRef](#)]
9. Bassil, E.; Ohto, M.A.; Esumi, T.; Tajima, H.; Zhu, Z.; Cagnac, O.; Belmonte, M.; Peleg, Z.; Yamaguchi, T.; Blumwald, E. The *Arabidopsis* intracellular Na⁺/H⁺ antiporters NHX5 and NHX6 are endosome associated and necessary for plant growth and development. *Plant Cell* **2011**, *23*, 224–239. [[CrossRef](#)]
10. Bassil, E.; Tajima, H.; Liang, Y.C.; Ohto, M.A.; Ushijima, K.; Nakano, R.; Esumi, T.; Coku, A.; Belmonte, M.; Blumwald, E. The *Arabidopsis* Na⁺/H⁺ antiporters NHX1 and NHX2 control vacuolar pH and K⁺ homeostasis to regulate growth, flower development, and reproduction *Plant Cell* **2011**, *23*, 4526–4526. *Plant Cell* **2011**, *23*, 4526.

11. Brown, R.S.; Sander, C.; Argos, P. The primary structure of transcription factor TFIIIA has 12 consecutive repeats. *FEBS Lett.* **1985**, *186*, 271–274. [[CrossRef](#)] [[PubMed](#)]
12. Miller, J.; McLachlan, A.D.; Klug, A. Repetitive zinc-binding domains in the protein transcription factor IIIA from *Xenopus* oocytes. *EMBO J.* **1985**, *4*, 1609–1614. [[CrossRef](#)] [[PubMed](#)]
13. Milla, M.A.; Townsend, J.; Chang, I.F.; Cushman, J.C. The *Arabidopsis* AtDi19 gene family encodes a novel type of Cys2/His2 zinc-finger protein implicated in ABA-independent dehydration, high-salinity stress and light signaling pathways. *Plant Mol. Biol.* **2006**, *61*, 13–30. [[CrossRef](#)] [[PubMed](#)]
14. Liu, W.X.; Zhang, F.C.; Zhang, W.Z.; Song, L.F.; Wu, W.H.; Chen, Y.F. *Arabidopsis* Di19 functions as a transcription factor and modulates PR1, PR2, and PR5 expression in response to drought stress. *Mol. Plant* **2013**, *6*, 1487–1502. [[CrossRef](#)]
15. Gosti, F.; Bertauche, N.; Vartanian, N.; Giraudat, J. Abscisic acid-dependent and -independent regulation of gene expression by progressive drought in *Arabidopsis thaliana*. *Mol. Gen. Genet. MGG* **1995**, *246*, 10–18. [[CrossRef](#)]
16. Feng, Z.J.; Cui, X.Y.; Cui, X.Y.; Chen, M.; Yang, G.X.; Ma, Y.Z.; He, G.Y.; Xu, Z.S. The soybean GmDi19-5 interacts with GmLEA3.1 and increases sensitivity of transgenic plants to abiotic stresses. *Front. Plant Sci.* **2015**, *6*, 179. [[CrossRef](#)]
17. Li, G.; Tai, F.J.; Zheng, Y.; Luo, J.; Gong, S.Y.; Zhang, Z.T.; Li, X.B. Two cotton Cys2/His2-type zinc-finger proteins, GhDi19-1 and GhDi19-2, are involved in plant response to salt/drought stress and abscisic acid signaling. *Plant Mol. Biol.* **2010**, *74*, 437–452. [[CrossRef](#)]
18. Zhang, X.; Cai, H.; Lu, M.; Wei, Q.; Xu, L.; Bo, C.; Ma, Q.; Zhao, Y.; Cheng, B. A maize stress-responsive Di19 transcription factor, ZmDi19-1, confers enhanced tolerance to salt in transgenic *Arabidopsis*. *Plant Cell Rep.* **2019**, *38*, 1563–1578. [[CrossRef](#)]
19. Li, S.; Xu, C.; Yang, Y.; Xia, G. Functional analysis of TaDi19A, a salt-responsive gene in wheat. *Plant Cell Environ.* **2010**, *33*, 117–129.
20. Wang, L.; Yu, C.; Xu, S.; Zhu, Y.; Huang, W. OsDi19-4 acts downstream of OsCDPK14 to positively regulate ABA response in rice. *Plant Cell Environ.* **2016**, *39*, 2740–2753. [[CrossRef](#)]
21. Wu, M.; Liu, H.; Gao, Y.; Shi, Y.; Pan, F.; Xiang, Y. The moso bamboo drought-induced 19 protein PheDi19-8 functions oppositely to its interacting partner, PheCDPK22, to modulate drought stress tolerance. *Plant Sci.* **2020**, *299*, 110605. [[CrossRef](#)] [[PubMed](#)]
22. Wu, C.; Lin, M.; Chen, F.; Chen, J.; Liu, S.; Yan, H.; Xiang, Y. Homologous drought-induced 19 proteins, PtDi19-2 and PtDi19-7, enhance drought tolerance in transgenic plants. *Int. J. Mol. Sci.* **2022**, *23*, 3371. [[CrossRef](#)] [[PubMed](#)]
23. Lata, C.; Gupta, S.; Prasad, M. Foxtail millet: A model crop for genetic and genomic studies in bioenergy grasses. *Crit. Rev. Biotechnol.* **2013**, *33*, 328–343. [[CrossRef](#)] [[PubMed](#)]
24. Peng, R.; Zhang, B. Foxtail millet: A new model for C₄ plants. *Trends Plant Sci.* **2021**, *26*, 199–201. [[CrossRef](#)]
25. Lu, H.; Zhang, J.; Liu, K.B.; Wu, N.; Li, Y.; Zhou, K.; Ye, M.; Zhang, T.; Zhang, H.; Yang, X.; et al. Earliest domestication of common millet (*Panicum miliaceum*) in East Asia extended to 10,000 years ago. *Proc. Natl. Acad. Sci. USA* **2009**, *106*, 7367–7372. [[CrossRef](#)] [[PubMed](#)]
26. Yang, X.; Wan, Z.; Perry, L.; Lu, H.; Wang, Q.; Zhao, C.; Li, J.; Xie, F.; Yu, J.; Cui, T.; et al. Early millet use in northern China. *Proc. Natl. Acad. Sci. USA* **2012**, *109*, 3726–3730. [[CrossRef](#)]
27. Liu, S.S.; Yang, R.; Liu, M.; Zhang, S.Z.; Yan, K.; Yang, G.D.; Huang, J.G.; Zheng, C.C.; Wu, C.A. PLATZ2 negatively regulates salt tolerance in *Arabidopsis* seedlings by directly suppressing the expression of the CBL4/SOS3 and CBL10/SCaBP8 genes. *J. Exp. Bot.* **2020**, *71*, 5589–5602. [[CrossRef](#)]
28. Xiao, S.; Wan, Y.; Zhang, L.; Tang, S.; Sui, Y.; Bai, Y.; Wang, Y.; Liu, M.; Fan, J.; Zhang, S.; et al. SiPLATZ12 transcript factor regulates multiple yield traits and salt tolerance in foxtail millet. *bioRxiv* **2022**. bioRxiv:498439.
29. Qin, L.X.; Li, Y.; Li, D.D.; Xu, W.L.; Zheng, Y.; Li, X.B. *Arabidopsis* drought-induced protein Di19-3 participates in plant response to drought and high salinity stresses. *Plant Mol. Biol.* **2014**, *86*, 609–625. [[CrossRef](#)] [[PubMed](#)]
30. Maitra Majee, S.; Sharma, E.; Singh, B.; Khurana, J.P. Drought-induced protein (Di19-3) plays a role in auxin signaling by interacting with IAA14 in *Arabidopsis*. *Plant Direct* **2020**, *4*, e00234. [[CrossRef](#)]
31. Wang, L.; Yu, C.; Chen, C.; He, C.; Zhu, Y.; Huang, W. Identification of rice Di19 family reveals OsDi19-4 involved in drought resistance. *Plant Cell Rep.* **2014**, *33*, 2047–2062. [[CrossRef](#)] [[PubMed](#)]
32. Qiu, Q.S.; Guo, Y.; Dietrich, M.A.; Schumaker, K.S.; Zhu, J.K. Regulation of SOS1, a plasma membrane Na⁺/H⁺ exchanger in *Arabidopsis thaliana*, by SOS2 and SOS3. *Proc. Natl. Acad. Sci. USA* **2002**, *99*, 8436–8441. [[CrossRef](#)]
33. Quan, R.; Lin, H.; Mendoza, I.; Zhang, Y.; Cao, W.; Yang, Y.; Shang, M.; Chen, S.; Pardo, J.M.; Guo, Y. SCaBP8/CBL10, a putative calcium sensor, interacts with the protein kinase SOS2 to protect *Arabidopsis* shoots from salt stress. *Plant Cell* **2007**, *19*, 1415–1431. [[CrossRef](#)] [[PubMed](#)]
34. Zhang, Y.; Linghu, J.; Wang, D.; Liu, X.; Yu, A.; Li, F.; Zhao, J.; Zhao, T. Foxtail millet CBL4 (SiCBL4) interacts with SiCIPK24, modulates plant salt stress tolerance. *Plant Mol. Biol.* **2017**, *35*, 634–646. [[CrossRef](#)]
35. Yan, J.; Yang, L.; Liu, Y.; Zhao, Y.; Han, T.; Miao, X.; Zhang, A. Calcineurin B-like protein 5 (SiCBL5) in *Setaria italica* enhances salt tolerance by regulating Na⁺ homeostasis. *Crop. J.* **2022**, *10*, 234–242. [[CrossRef](#)]
36. Barragán, V.; Leidi, E.O.; Andrés, Z.; Rubio, L.; De Luca, A.; Fernández, J.A.; Cubero, B.; Pardo, J.M. Ion exchangers NHX1 and NHX2 mediate active potassium uptake into vacuoles to regulate cell turgor and stomatal function in *Arabidopsis*. *Plant Cell* **2012**, *24*, 1127–1142. [[CrossRef](#)] [[PubMed](#)]
37. Bassil, E.; Coku, A.; Blumwald, E. Cellular ion homeostasis: Emerging roles of intracellular NHX Na⁺/H⁺ antiporters in plant growth and development. *J. Exp. Bot.* **2012**, *63*, 5727–5740. [[CrossRef](#)]

38. Wu, X.; Ebine, K.; Ueda, T.; Qiu, Q.S. AtNHX5 and AtNHX6 are required for the subcellular localization of the SNARE complex that mediates the trafficking of seed storage proteins in *Arabidopsis*. *PLoS ONE* **2016**, *11*, e0151658. [[CrossRef](#)]
39. Reguera, M.; Bassil, E.; Tajima, H.; Wimmer, M.; Chanoca, A.; Otegui, M.S.; Paris, N.; Blumwald, E. pH regulation by NHX-Type antiporters is required for receptor-mediated protein trafficking to the vacuole in *Arabidopsis*. *Plant Cell* **2015**, *27*, 1200–1217. [[CrossRef](#)]
40. Zhang, L.; Ren, Y.; Xu, Q.; Wan, Y.; Zhang, S.; Yang, G.; Huang, J.; Yan, K.; Zheng, C.; Wu, C. SiCEP3, a C-terminally encoded peptide from *Setaria italica*, promotes ABA import and signaling. *J. Exp. Bot.* **2021**, *72*, 6260–6273. [[CrossRef](#)]
41. Yu, Z.; Zhang, D.; Xu, Y.; Jin, S.; Zhang, L.; Zhang, S.; Yang, G.; Huang, J.; Yan, K.; Wu, C.; et al. CEPR2 phosphorylates and accelerates the degradation of PYR/PYLs in *Arabidopsis*. *J. Exp. Bot.* **2019**, *70*, 5457–5469. [[CrossRef](#)]
42. Xu, Y.; Yu, Z.; Zhang, D.; Huang, J.; Wu, C.; Yang, G.; Yan, K.; Zhang, S.; Zheng, C. CYSTM, a novel non-secreted Cysteine-rich peptide family, involved in environmental stresses in *Arabidopsis thaliana*. *Plant Cell Physiol.* **2018**, *59*, 423–438. [[CrossRef](#)] [[PubMed](#)]
43. Clough, S.J.; Bent, A.F. Floral dip: A simplified method for *Agrobacterium*-mediated transformation of *Arabidopsis thaliana*. *Plant J.* **1998**, *16*, 735–743. [[CrossRef](#)] [[PubMed](#)]
44. Li, W.; Chen, M.; Wang, E.; Hu, L.; Hawkesford, M.J.; Zhong, L.; Chen, Z.; Xu, Z.; Li, L.; Zhou, Y.; et al. Genome-wide analysis of autophagy-associated genes in foxtail millet (*Setaria italica* L.) and characterization of the function of SiATG8a in conferring tolerance to nitrogen starvation in rice. *BMC Genom.* **2016**, *17*, 797. [[CrossRef](#)] [[PubMed](#)]

Disclaimer/Publisher’s Note: The statements, opinions and data contained in all publications are solely those of the individual author(s) and contributor(s) and not of MDPI and/or the editor(s). MDPI and/or the editor(s) disclaim responsibility for any injury to people or property resulting from any ideas, methods, instructions or products referred to in the content.